IONOSPHERIC EFFECTS UPON A SATELLITE NAVIGATION SYSTEM AT MARS

Michael Mendillo[1], Xiaoqing Pi[2], Steven Smith[1], Carlos Martinis[1], Jody Wilson[1], and David Hinson[3]

[1]Center for Space Physics
Boston University
Boston, MA 02215

[2]Jet Propulsion Laboratory
California Institute of Technology
Pasadena, CA 91109

[3]Department of Electrical Engineering
Stanford University
Stanford, CA 94305

ABSTRACT

Trans-ionospheric radio propagation effects resulting in ranging errors are examined for a potential orbital network of communications and navigational satellites at Mars. Using recent results from the radio science experiment onboard the Mars Global Surveyor (MGS) spacecraft and a photochemical model of Mars' ionosphere, we study the total electron content at Mars to investigate how its latitude, local time and solar cycle patterns would contribute to errors in positioning on the planet. For UHF transmission frequencies similar to those used for the terrestrial Global Positioning System (GPS) satellites, upper limits to the magnitude and variability of the martian ionosphere (TEC < ~few x 10^{16} el m^{-2}) would not be of concern unless extremely precise positional information were required (<1 meter). The impact of the ionosphere would be greater at lower frequencies, and indeed such effects could be used as a diagnostic for the global structure of Mars' ionosphere, much in the same way as GPS measurements are used in terrestrial ionospheric physics.

Submitted to RADIO SCIENCE, 10 July 2003.

I. INTRODUCTION: The Terrestrial Ionosphere and GPS Impacts

A planet's ionosphere imposes a delay upon the radio transmissions from an orbiting artificial satellite to a ground receiving station, thus leading to ranging errors in systems designed for precise positioning. This is a well-studied effect on Earth for the Global Positioning System (GPS) used in an ever-increasing spectrum of civilian and military applications. Illustrated schematically in Figure 1(a) is the augmented GPS system use for air travel across the continental US (CONUS). The terrestrial ionosphere exhibits dramatic variations in latitude and local time across CONUS, and especially so during periods of solar and geomagnetic activity. Technically, the ionospheric delay effect could be eliminated by operating the system with dual-frequency signals transmitted by the satellites. Otherwise, either real-time measurements of the ionosphere or reliable models of its temporal and spatially dependent behavior are needed to correct for "group path delay effects" that could lead to errors in the determination of aircraft location.

For the terrestrial case, 24 GPS satellites are configured at an altitude of about 20,200 km in 6 orbital planes in order to have at least 4 satellites available at any time from any place to determine a receiver's location. The slanted paths from the receivers to the satellites thus traverse great distances and sample the ionosphere in several directions. The ionospheric parameter of relevance is the integral of electron density along these paths (s), called the slant total electron content,

$$\text{STEC} = \int_r^s N_e(s)ds \qquad (1)$$

While the limits of the integral in equation (1) extend from the receiver to the satellite height, in practice most of the ionosphere is well below GPS heights, and thus an integral to ~2000 km captures most of the effects of interest. This is fortunate from the perspective of modeling since ionospheric structure to such altitudes involves a set of physical processes and computational

methods somewhat different from those needed to model plasma in the inner magnetosphere (or plasmasphere) where the GPS satellites actually reside. To reduce the problem further, it is useful to consider the ionosphere to be spatially constant over the region traversed by a ray path from the ground to ~2000 km, and this is not a bad assumption if the zenith angle (χ) to the satellite is not too large, e.g., < 60^o. This allows the local ionosphere to be represented by a single electron density profile with a single vertically integrated total electron content (TEC). For such conditions, the relation between STEC and TEC is simply

$$\mathrm{STEC} = \mathrm{TEC}\sec(\chi) \qquad (2)$$

and the vertical TEC parameter becomes the target to observe or model. The units chosen to describe TEC are most often in metric column contents of 10^{16} el m^{-2}, called a "TEC unit" or TECU. The lowest TEC values on Earth (~2 TECU) occur during winter nighttimes at sub-auroral latitudes during solar minimum, and the largest ones (~200 TECU) can be found during solar maximum periods at latitudes within 20^o of the geomagnetic equator, in regions called the Equatorial Ionization Anomaly (EIA) or the Appleton Anomaly crests (see Rishbeth and Garriott, 1969). For the GPS satellite L1 frequency (1.57542 GHz), such TEC values correspond to ~0.32 to ~32 meters of vertical equivalent range errors, respectively. Such values are of considerable concern to precise positioning and navigation systems, and thus considerable research efforts are underway in real-time monitoring of the ionosphere, numerical modeling of its behavior, and methods of forecasting for both geomagnetically quiet and disturbed periods (e.g., Pi *et al*., 2003).

II. The Case at Mars.

The operational system illustrated in Figure 1(a) offers ideas to examine in plans for upcoming explorations of Mars. With a series of orbiters, landers and rovers planned for the upcoming decades, including sample gathering and return missions, there is an obvious need for positioning and navigation of, as well as communications between, spacecraft and vehicles on the surface of Mars. Requirements are far more rigorous than used in NASA's initial attempts to explore the planet's surface with the Viking Landers in 1976. Moreover, several international programs

(both joint and independent from US plans) are underway, and thus the overall problem of positioning and communications could become rather complex. In Figure 1(b) we show an illustration of concepts being discussed for Mars, ideas not too dissimilar from those proposed in the 1970s that resulted in the now operational GPS systems on Earth. All of the proposed solutions involve some sort of multi-satellite network, with the eventual design accepted for the Mars Communications and Navigation (MC&N) system still very much under study (e.g., Cesarone *et al*., 1999; Ely et al., 1999; Hastrup *et al*., 1999).

To illustrate the type of ionospheric structure that would be of concern to any MC&N system, we show in Figure 2 several examples of $N_e(h)$ profiles obtained from the radio science experiment (Hinson *et al*., 2001) onboard the Mars Global Surveyor (MGS) satellite. The observational parameters for these three initial periods of MGS ionospheric experiments are given in Table 1. Due to the geometrical limitations imposed by radio occultation experiments between the MGS orbit about Mars and Earth's location, these samplings of the martian ionosphere all refer to high latitudes and early local times in the northern hemisphere. There are several features to note. Firstly, most of the ionosphere falls within the ~100 to ~200 km altitude range, about a factor of ten smaller than the physical extent of the terrestrial ionosphere and, on a percentage basis, ~10% vs. 30% of their respective planetary radii. The peak electron density on Mars occurs near 135 km, with a secondary peak near 110 km. At these altitudes, the density of the neutral atmosphere is comparable to that found in the terrestrial E-region, and thus photochemical processes (i.e., solar production, chemical loss and no plasma transport) are sufficient to describe the first-order behavior of Mars' ionosphere (as described recently in Mendillo *et al*. (2003), and references therein).

There is quite a bit of variability in the profiles in Figure 2, both in the electron density values and in the heights of their maxima. Some of the variability in height arises from longitude effects in the neutral atmosphere at the same local times, as the MGS occultation paths sample several locations on Mars during a day (Bougher *et al*., 2001). Daily changes in solar flux account for most of the variability in electron density, as shown in Mendillo *et al*. (2003) and Martinis *et al*. (2003).

To determine TEC values from the $N_e(h)$ profiles in a consistent way, we performed the integration in Equation (2) from 100 km to 200 km. There are very low electron density values below, and especially above, these heights that cannot be retrieved accurately via the inversion of MGS radio occultation measurements, and these would contribute to the actual TEC value at a given time. The topside ionosphere at Mars often exhibits a sharp termination called "the ionopause" (Kliore, 1992; Vignes et al., 2000) in the 300-500 km region, and thus an additional topside segment with $N_e < \sim 10^{10}$ el m^{-3} would contribute to the true TEC integral. Holding these topside and bottomside corrections aside for the moment, the major contributions to TEC are shown for the three data periods in Figure 3. There is a remarkable consistency in the TEC values and their ranges. The value of ~0.42 TECU is thus representative of this ~03-04 LT period and latitude range on Mars. Adding small corrections for the contributions below 100 km (~0.02 TECU) and above ~200 km (~0.2 TECU), gives us an overall estimate of, perhaps, 0.7 TECU for the conditions sampled.

To the terrestrial ionospheric physicist, such a small value is within the error of terrestrial TEC values, and certainly of little consequence for GPS applications. What are the implications for the situation on Mars? To address this issue quantitatively, we show in Figure 4 the relationship between range error (ΔR) and TEC magnitude derived from the radio time retardation dependence with frequency relationship (Hargreaves, 1992),

$$\Delta R = 0.403 \frac{TEC}{f^2} \qquad (4)$$

where TEC is measured in TECU (10^{16} el m^{-2}), f is in GHz, and ΔR is in meters.

If a Mars Communications and Navigation system were to adopt GPS frequencies, the martian ionosphere with ~ 1 TECU would cause about 0.3 m of position error, probably of little consequence to mission managers. For an UHF signal of 400 MHz, however, the martian case of ~1 TECU corresponds to a range error of about 2.5 meters. This number would need to be multiplied by factors up to ~3 for lower elevation views needed for the positioning of surface

rovers, for example. As part of the planning process for a MC&N system, for which estimates of ionospheric range delays are an important element, it is useful to ask how restrictive a view of Mars' ionosphere comes from the profiles in Figure 2 and their TEC values in Figure 3. To do this, we turn to modeling estimates.

III. Simulations of the Mars Ionosphere for Total Electron Content Estimates

All of the $N_e(h)$ profiles shown in Figure 2 were obtained under solstice conditions on Mars, at latitudes with sunlight present at large zenith angles for the full day. For such a case, the diurnal variation of a photochemical layer is not too dramatic. This can be shown using the model described in Martinis *et al*. (2003), one that used the standard photochemical equations and neutral atmosphere profiles described in Fox *et al*. (1995). The results are given in Figure 5. In the top panel, the peak electron density is shown for the average solar conditions for 24-31 December 1998, the initial period of MGS radio science occultation observations. Simulation results for two locations are given: latitude 67° N where the MGS data were taken near 04 LT (shown by the solid line), and at 24° N, the latitude of the sub-solar point on Mars, where the maximum electron densities on the planet would occur (shown by the dashed line). The first feature to notice is the very mild gradient in latitude for peak electron density. The noontime value of N_{max} for a solar zenith angle of 0^o is only slightly higher than the noontime value for a SZA of 42^o at the high latitude site. This reflects the small dependence upon zenith angle in the Chapman equations for a photochemical (α-Chapman) layer.

$$N_{max} = [(P/\alpha) \cos\chi]^{0.5} \qquad (5)$$

where P is the peak production rate for an overhead sun and α the recombination coefficient (for an in-depth discussion of this point, see recent terrestrial E-layer model of Titheridge (2000)). For the two simulation values of N_{max} shown in Figure 5, a cosine fit results in an exponent equal to 0.55, essentially consistent with the simple theory embodied in equation (5).

At the sub-solar site (representative of all low-to-mid latitudes for diurnal behavior), the familiar rise and decay of a photochemical layer at sunrise and sunset are seen in the dashed-line curve.

The diurnal variation is over a factor of 40 at this location. At the "arctic circle" location sampled by MGS, however, the Sun does not set and thus the photochemical layer persists at all local times. The diurnal variation there is only a factor of 4. The value of N_{max} at ~04 LT obtained from MGS is shown by the diamond symbol and falls somewhat below the simulation results (solid line). This is due to several simplifying assumptions used in the model, the primary one being a constant neutral atmosphere in space and time over the planet. Yet, the results do address satisfactorily the specific question we posed, namely, the relationship between the MGS observations at high latitudes and early local times to the maximum levels of ionospheric densities elsewhere on the planet.

The lower panel in Figure 5 gives the simulation results for total electron content (TEC) at the two latitudes. As would be expected, the diurnal behavior for TEC is similar to that for peak density, and the diurnal range is again nearly a factor of four. The model's small TEC shortfall at the comparison point with the MGS observations occurs from the same limitations described above for peak density. In addition, there is considerable uncertainty for the photo-electron secondary ionization rate that contributes to bottomside peak densities that contribute to TEC (see Martinis *et al.* (2003), for full model details). Still, the agreement is rather good and we feel confident in using the model to estimate the ranges possible for the maximum TEC on Mars throughout a typical solar cycle. To do this, we stay at the sub-solar point and run the model for the extreme cases of Mars at perihelion and aphelion at times of solar minimum and maximum. The solar min/max neutral atmospheres come from Fox *et al*., (1995) and the solar irradiance patterns from the SOLAR 2000 model of Tobiska et al. (2000). The results of these four case studies are shown in Figure 6. The full solar cycle range for daytime TEC in the 100-200 km altitude range is thus ~0.7 to ~1.4 TECU. As pointed out earlier, on Earth the variation of TEC over a solar cycle would be one to two orders of magnitude larger, not so much due to the Earth's closer distance to the Sun, but to the nature of a non-photochemical layer (F2) providing the major contribution to the TEC integral.

III. Changes in The Equivalent Slab Thickness of the Martian Ionosphere

The representation of an ionosphere by its so-called equivalent slab thickness (τ) is illustrated in Figure 7. If the TEC were to result from a layer with electron density uniformly equal to the peak density, the resulting slab thickness can be a useful way to describe the first order shape (i.e., breadth) of the $N_e(h)$ profile. In the terrestrial case, τ varies in space and time far less dramatically than either of its parameters (N_{max} and TEC), and thus empirical models for τ have been used for regional and global specifications of TEC when ionosonde measurements of N_{max} are the only observable available (Fox *et al.*, 1991). Since the ionospheric database for Mars is far from regional or global, it is instructive to examine how slab thickness on Mars represents the local ionosphere at the MGS measurement points. For the three datasets shown in Figure 2, the resulting slab thickness values are shown in histogram form in Figure 8.

Comparing the TEC statistics in Figures 3 (that show limited variability) with the more variable slab thickness results in Figure 6 suggests that the major changes in shape of the ionosphere on Mars are related to changes in N_{max}. Thus, in Figure 9 we explore the correlation of slab thickness versus peak density. There is a clear trend of the ionosphere becoming thinner as the peak density increases. The trend is rather pronounced in the December 1998 set of MGS profiles, but also clearly apparent in the March 1999 and December 2000 data as well.

The causes of such integral-preserving distortions of the $N_e(h)$ profiles are not obvious. Given that plasma diffusion is not important at these altitudes, the photochemical regime must be influenced by either solar or neutral atmosphere effects. In Figure 10, we show the effects of solar input for the extreme cases of Mars at aphelion during solar minimum versus perihelion during solar maximum (i.e., the $N_e(h)$ profiles used to generate the second and fourth TEC values shown in Figure 6). For photochemical-only processes, it is clear that a $N_e(h)$ profile *broadens* with increasing N_{max}, contrary to the pattern shown in Figure 9. Other causes, such as neutral atmosphere dynamics, need to be examined to understand the $N_e(h)$ integral-preserving distortion effects portrayed in Figure 9.

IV. SUMMARY AND CONCLUSIONS

We have examined the first three sets of electron density versus altitude profiles obtained from the MGS radio occultation experiment with the goal of describing their integrated values, or total electron content (TEC), as a way to assess the impact of Mars' ionosphere on potential satellite-based position and navigation systems. The MGS datasets all refer to early local times at high latitudes, arising from solar illumination at high zenith angles, and thus modeling studies were conducted to relate these local measurements to more global morphologies. Photochemical model estimates for the maximum TEC possible on the planet, namely at the sub-solar point at perihelion under solar maximum conditions, indicated at most ~2-3 vertical TEC units (10^{16} el m^{-2}). If sampled along slanted ray-paths from orbit to ground, or by satellite-to-satellite ray-paths horizontally through the ionosphere, the TEC encountered might be a factor of 3 larger. For such upper limit estimates, and for a navigation system using the current GHz frequencies employed for the terrestrial GPS system, range errors would be less than 2 meters. This may be a concern to mission planners, but other uncertainties in precise positioning on Mars might be larger. If the radio beacon frequencies selected for a Mars Communications and Navigation satellite network were much lower (i.e., in the UHF band), then ionospheric corrections would be of greater relevance. If a dual frequency MC&N system were put into operation at Mars, issues of ionospheric TEC corrections are avoided. Yet, for either solution, it is important to realize that the transmissions themselves would provide a new and extremely valuable diagnostic of the martian ionosphere on a global and continuous basis, providing critical input to ionospheric models and upper atmospheric science, as the current GPS system does on Earth.

ACKNOWLEDGEMENTS.

The efforts at Boston University were supported, in part, by a grant from the Mars Data Analysis Program, and by seed research funds from the Center for Space Physics. At Stanford University, support for this work came from the Mars Global Surveyor Program. The research conducted at the Jet Propulsion Laboratory, California Institute of Technology, is under a contract with National Aeronautics and Space Administration.

FIGURE CAPTIONS.

Figure 1. Panel(a). An illustration of the use of the Global Positioning System (GPS) satellites for precise location and navigation of aircraft over the continental US (CONUS). Satellite radio transmissions to aircraft and ground sites traverse the terrestrial ionosphere and suffer retardation effects that lead to range errors, if not corrected for the total electron content (TEC) of the ionosphere along each raypath. (Figure courtesy of the Federal Aviation Administration.)
Panel (b). A schematic illustration of a proposed Mars Network for communications and navigation. Several such concepts are under study, and ionospheric corrections for the TEC on Mars depend on the final selection of frequencies to be used. (Figure courtesy of NASA/JPL.)

Figure 2. Electron density vs. altitude profiles from the radio science experiment onboard the Mars Global Surveyor satellite. See Table 1 for observational specifics. For each of these three periods, the total electron content (TEC) parameter is formed by the vertical integration of the profiles shown.

Figure 3. The distribution of martian TEC values from the three $N_e(h)$ datasets shown in Figure 2.

Figure 4. Calculations of ionospherically imposed range errors for vertical TEC versus the frequency used in a satellite navigation system. The arrows indicate a typical UHF (400 MHz) choice, as well as the L1 and L2 frequencies of the terrestrial GPS system.

Figure 5. Photochemical model results for the peak electron density (top panel) and total electron content (lower panel) used to place MGS observations in December 1998 into the context of diurnal and latitude behavior on the planet. The solid lines give simulation results at the latitude of MGS data, and dashed lines give results for the sub-solar latitude. In both panels, the diamond symbol represents the average value for N_{max} and TEC obtained from the left panel in Figure 2. (See text)

Figure 6. Model results for noontime ionospheric TEC in the altitude range 100-200 km at the sub-solar latitude on Mars, for aphelion/perihelion positions during solar min/max conditions.

Figure 7. Illustration of three parameters used to characterize an ionospheric Ne(h) profile: N_{max}, TEC and equivalent slab thickness τ.

Figure 8. Distribution of the equivalent slab thickness values for Mars' ionosphere derived from the three sets of MGS data shown in Figure 2.

Figure 9. Behavior of equivalent slab thickness (τ) on Mars versus the peak electron density (N_{max}) for the three datasets in Figure 2.

Figure 10. Model results showing $N_e(h)$ profile shape changes at the sub-solar point for the extreme cases of Mars at aphelion at solar minimum versus perihelion at solar maximum.

REFERENCES

Appleton, E., Global morphology of the E- and F1-layers of the ionosphere, J. Atmosph. Terr. Phys., 15, 9-12, 1959.

Bougher, S.W., S. Engel, D.P. Hinson, and J.M. Forbes, Mars Global Surveyor Radio Science electron density profiles: Neutral atmosphere implications, Geophys. Res. Lett., 28, 3091-3094, 2001.Cesarone, R. J., R. C. Hastrup, D. J. Bell, D. T. Lyons and K. G. Nelson, Architectural Design for a Mars Communications & Navigation Orbital Infrastructure, *the AAS/AIAA Astrodynamics Specialist Conference*, Girwood, Alaska, August 16-19, 1999.

Ely, T. A., R. Anderson, Y. E. Bar-Sever, D. Bell, J. Guinn, M. Jah, P. Kallemeyn, E. Levene, L. Romans and S. Wu, Mars Network Constellation Design Drivers and Strategies, *the AAS/AIAA Astrodynamics Specialist Conference*, Girwood, Alaska, August 16-19, 1999.

Fox, J. L., P. Zhou, and S. W. Bougher, The Martian Thermosphere/Ionosphere at High and Low Solar Activities, Adv. Space Res., 17(11) 203-218, 1995.

Fox, M. W., M. Mendillo and J. A. Klobuchar, Ionospheric equivalent slab thickness and its modeling applications, Radio Sci., 26, 429-438, 1991.

Hargreaves, J. K., The Solar-Terrestrial Environment, Cambridge University Press, 1992.

Hastrup, R. C., R. J. Cesarone, J. M. Srinivasan and D. D. Morabito, Mars Comm/Nav MicroSat Network, *the 13th AIAA/USU Conference on Small Satellites*, Logan, Utah, August 23-26, 1999.

Hinson, D. P., G. L. Tyler, J. L. Hollingsworth, and R. J. Wilson, Radio occultation measurements of forced atmospheric waves on Mars, J. Geophys. Res., 106, 1463, 2001.

Kliore, A. J., Radio occultation observations of the ionospheres of Mars and Venus, Geophysical Monograph 66, 265-276, American Geophysical Union, 1992.

Martinis C., J. Wilson, and M. Mendillo, Modeling day-to-day ionospheric variability on Mars, submitted to J. Geophys. Res., April (2003).

Mendillo, M., S.M. Smith, H. Rishbeth, and D.P. Hinson, Simultaenous ionospheric variability on Earth and Mars, submitted to J. Geophys. Res., April (2003).

Pi, X., C. Wang, G. A. Hajj, G. Rosen, B. D. Wilson, and G. J. Bailey, Estimation of EB drift using a global assimilative ionospheric model: An observation system simulation experiment, J. Geophys. Res., *108*, 1075, 2003.

Rishbeth, H. and O. K. Garriott, Introduction to Ionospheric Physics, Academic Press, 1969.

Titheridge, J. E., Modelling the peak of the ionospheric E-layer, J. Atmosph. Solar Terr. Phys., 62, 93-114, 2000.

Vignes, D., C. Mazelle, H. Rme, M.H. Acuña, J.E.P. Connerney, R.P. Lin, D.L. Mitchell, P. Cloutier, D.H. Crider, N.F. Ness, The solar wind interaction with Mars: Locations and shapes of the bow shock and the magnetic pile-up boundary from the observations of the MAG/ER experiment onboard Mars Global Surveyor, Geophys. Res. Lett., *27*, No. 1, 49-52, 2000.

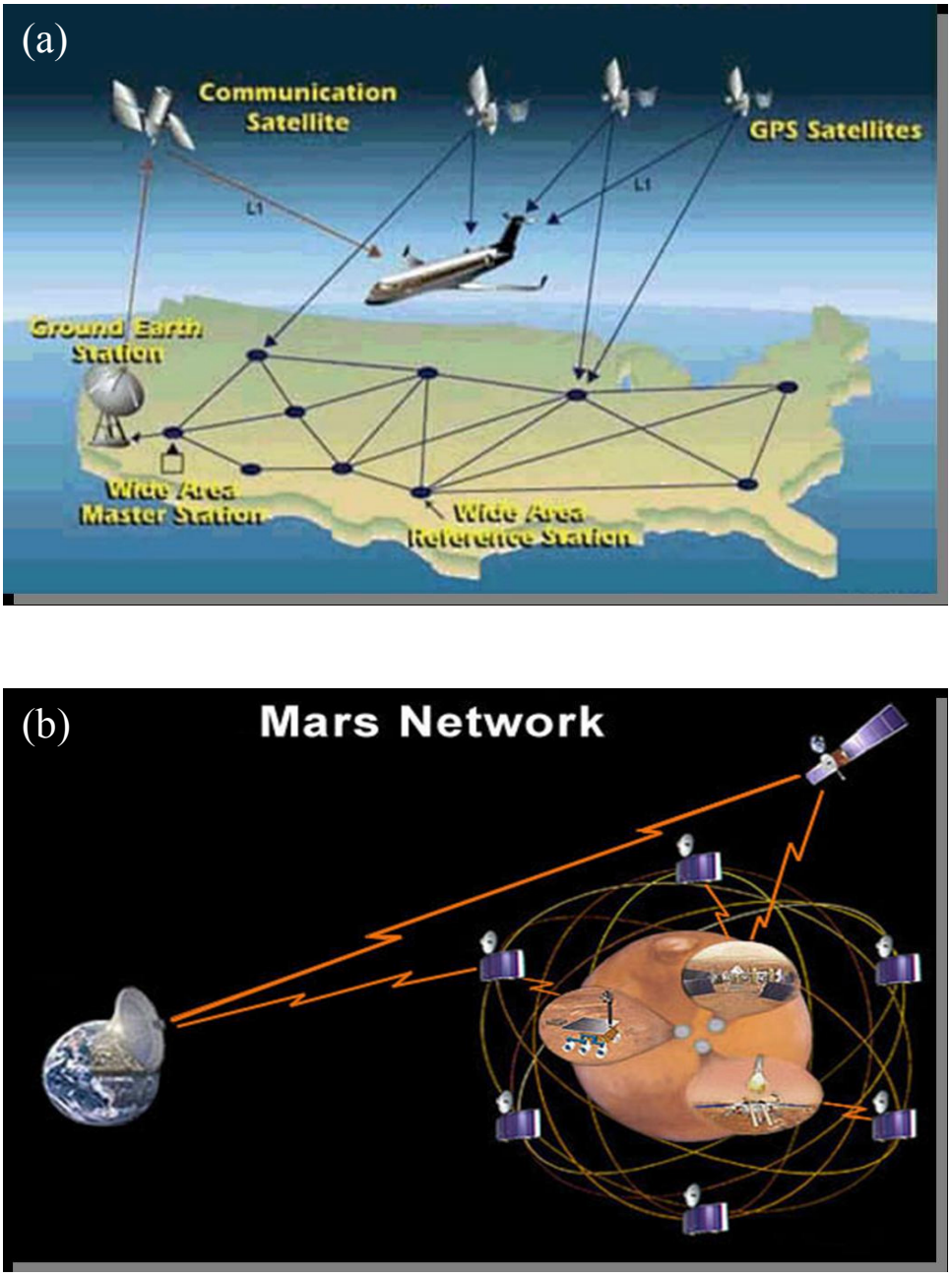

Figure 1. Panel(a). An illustration of the use of the Global Positioning System (GPS) satellites for precise location and navigation of aircraft over the continental US (CONUS). Satellite radio transmissions to aircraft and ground sites traverse the terrestrial ionosphere and suffer retardation effects that lead to range errors, if not corrected for the total electron content (TEC) of the ionosphere along each raypath. (Figure courtesy of the Federal Aviation Administration.)
Panel (b). A schematic illustration of a proposed Mars Network for communications and navigation. Several such concepts are under study, and ionospheric corrections for the TEC on Mars depend on the final selection of frequencies to be used. (Figure courtesy of NASA/JPL.)

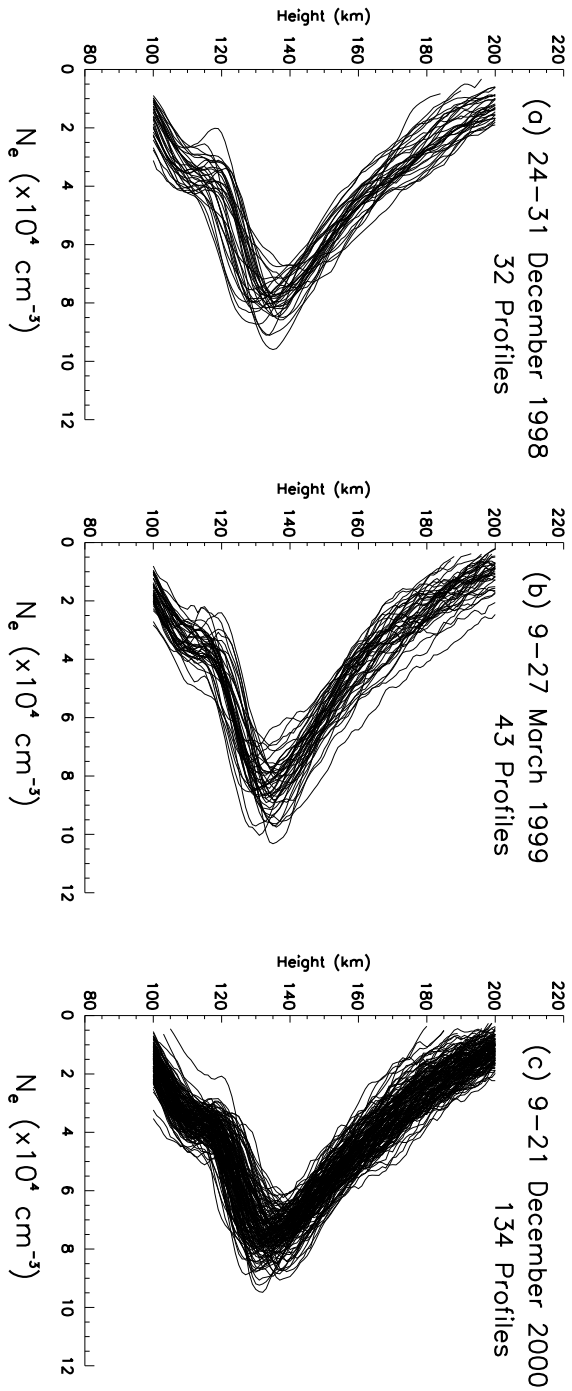

Figure 2. Electron density vs. altitude profiles from the radio science experiment onboard the Mars Global Surveyor satellite. See Table 1 for observational specifics. For each of these three periods, the total electron content (TEC) parameter is formed by the vertical integration of the profiles shown.

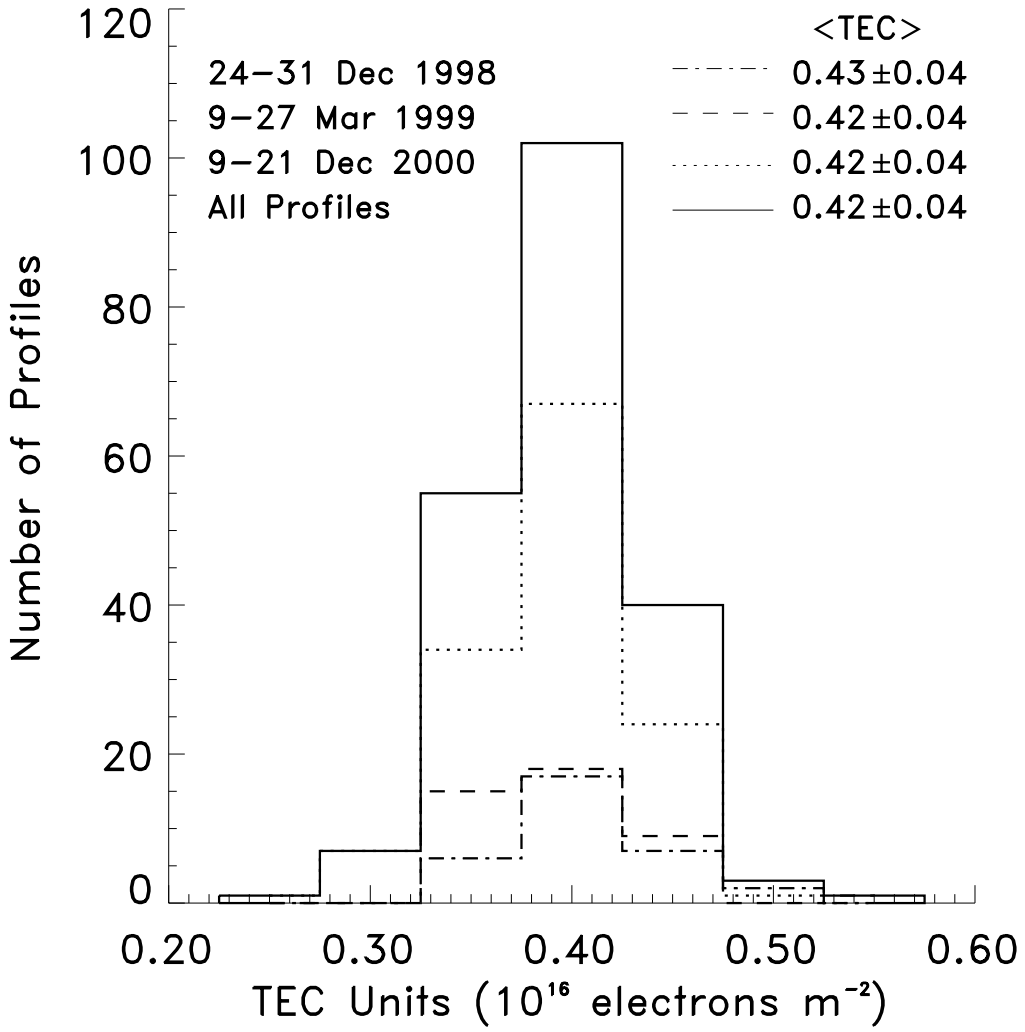

Figure 3. The distribution of martian TEC values from the three $N_e(h)$ datasets shown in Figure 2.

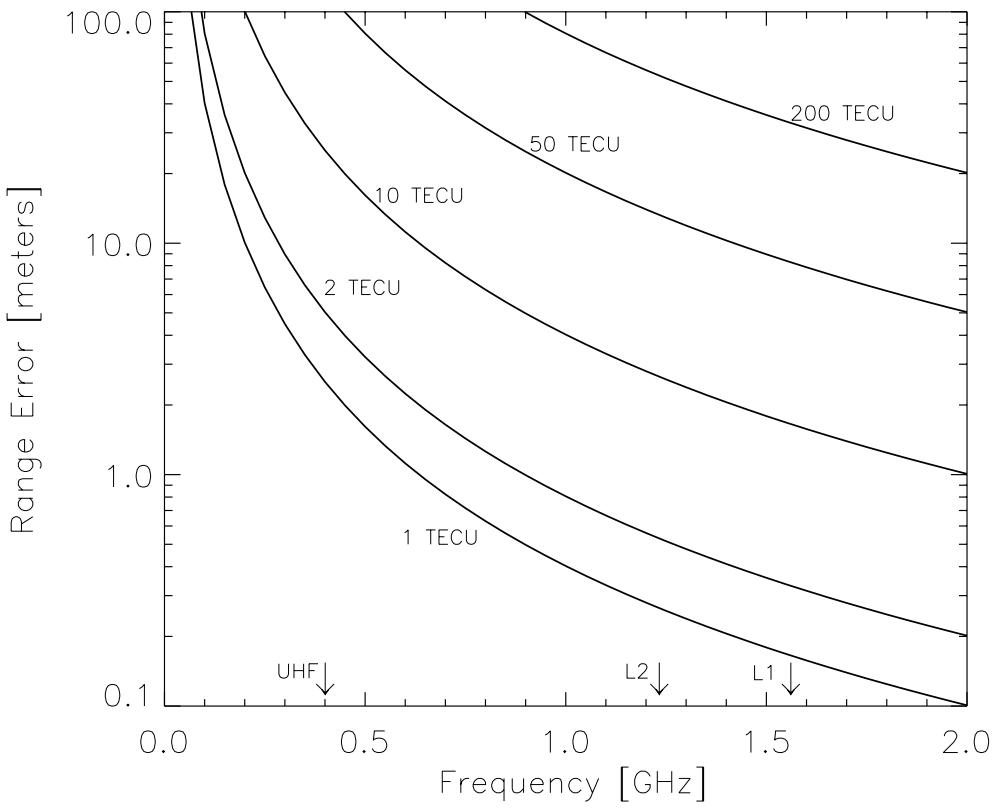

Figure 4. Calculations of ionospherically imposed range errors for vertical TEC versus the frequency used in a satellite navigation system. The arrows indicate a typical UHF (400 MHz) choice, as well as the L1 and L2 frequencies of the terrestrial GPS system.

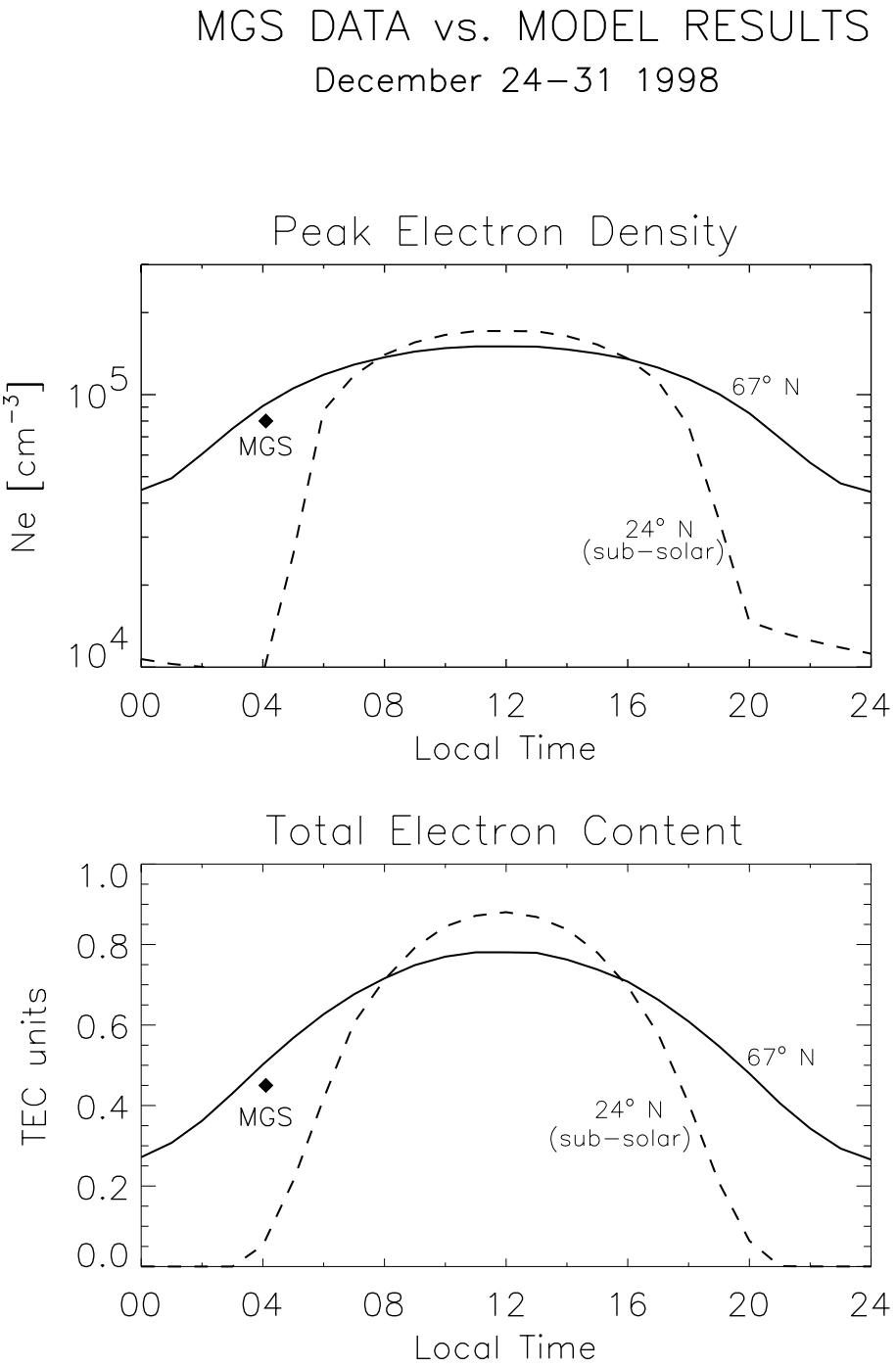

Figure 5. Photochemical model results for the peak electron density (top panel) and total electron content (lower panel) used to place MGS observations in December 1998 into the context of diurnal and latitude behavior on the planet. The solid lines give simulation results at the latitude of MGS data, and dashed lines give results for the sub-solar latitude. In both panels, the diamond symbol represents the average value for N_{max} and TEC obtained from the left panel in Figure 2. (See text)

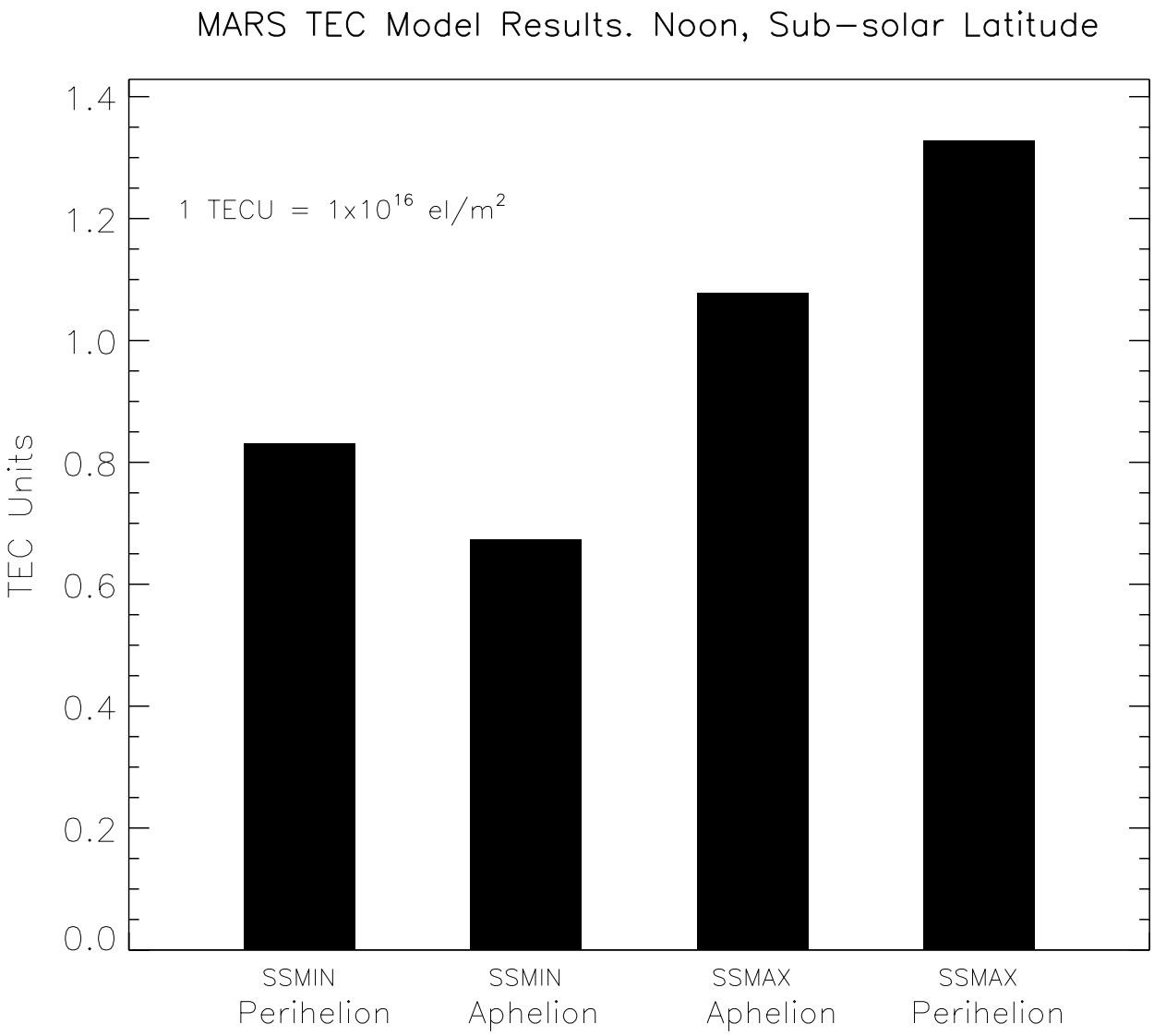

Figure 6. Model results for noontime ionospheric TEC in the altitude range 100-200 km at the sub-solar latitude on Mars, for aphelion/perihelion positions during solar min/max conditions.

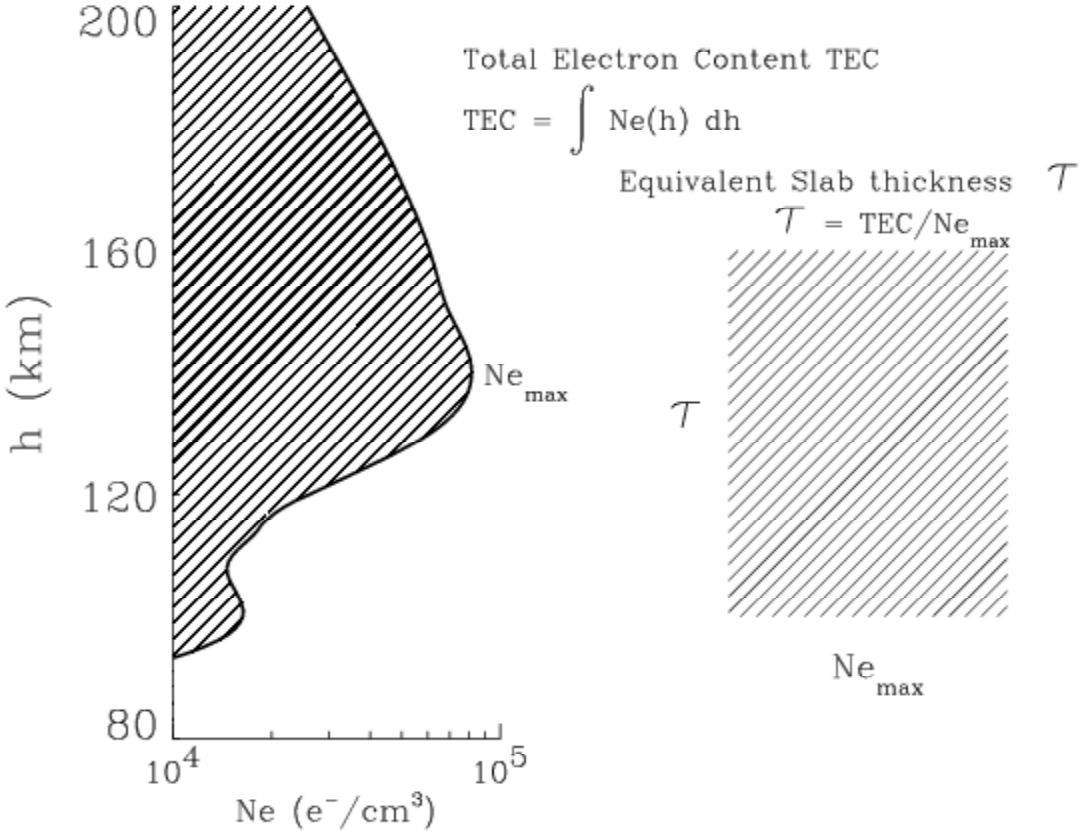

Figure 7. Illustration of three parameters used to characterize an ionospheric $N_e(h)$ profile: N_{max}, TEC and equivalent slab thickness τ.

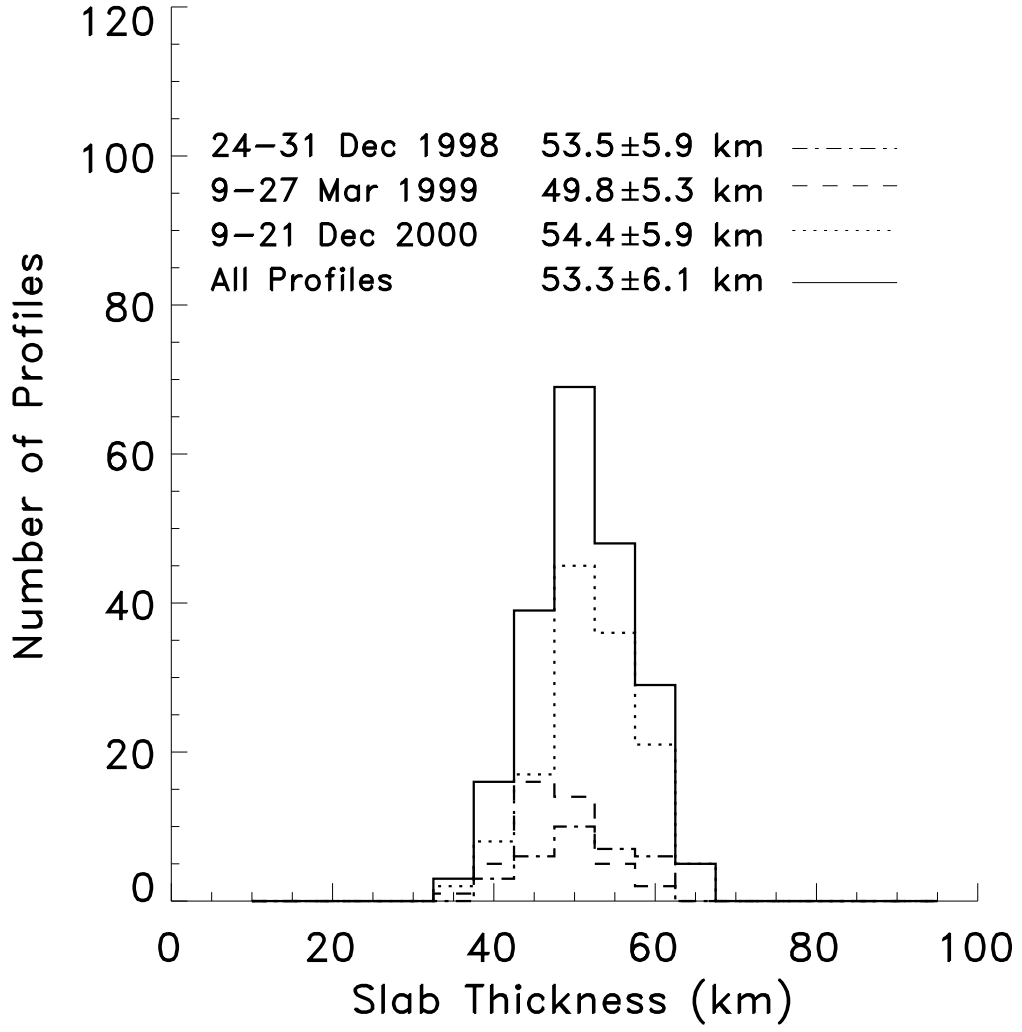

Figure 8. Distribution of the equivalent slab thickness values for Mars' ionosphere derived from the three sets of MGS data shown in Figure 2.

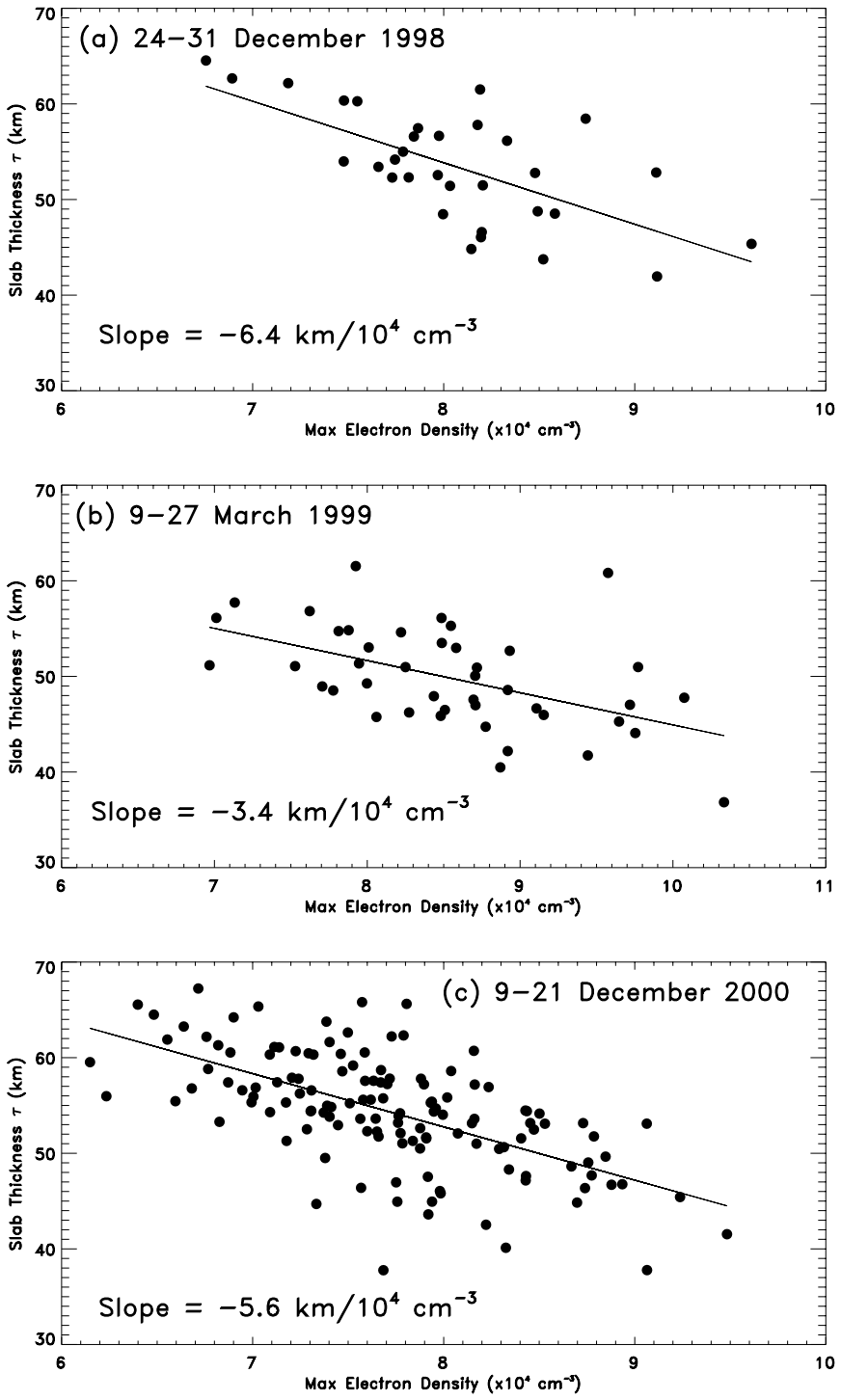

Figure 9. Behavior of equivalent slab thickness (τ) on Mars versus the peak electron density (N_{max}) for the three datasets in Figure 2.

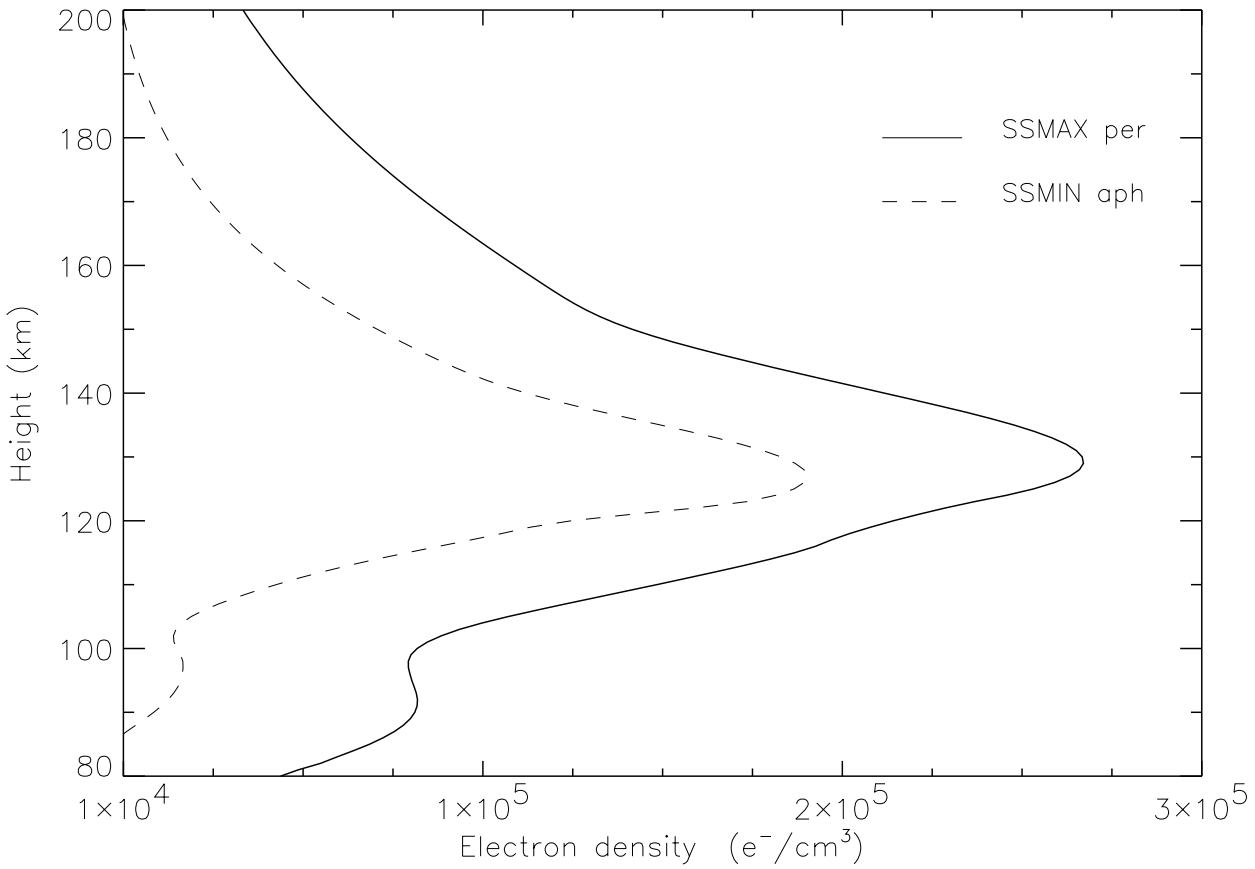

Figure 10. Model results showing $N_e(h)$ profile shape changes at the sub-solar point for the extreme cases of Mars at aphelion at solar minimum versus perihelion at solar maximum.

Table 1. MGS/Radio Science ionospheric profiles for the three periods of study.

Date	# of Profiles	Latitude Coverage	Longitude Coverage	Local Time (hrs)	Solar Zenith Angle	Ls*
24 – 31 Dec 1998	32	64.7˚ – 67.3˚	All	4.3 – 3.3	78.4˚ – 80.8˚	74.1˚ – 77.3˚
9, 11 – 27 Mar 1999	43	73.3˚ – 69.7˚	26.5˚ – 273.0˚	3.6 – 4.1	76.5˚ – 77.8˚	107.6˚ – 115.9˚
9 – 21 Dec 2000	134	67.5˚ – 69.6˚	All	2.8 – 2.8	80.5˚ – 82.2˚	86.8˚ – 92.5˚

* The solar longitude (Ls) is the angular measure of the orbital position of Mars about the sun (Ls = 0˚ or 180˚ at equinox; Ls = 90˚ at northern summer solstice; Ls = 270˚ at southern summer solstice).